SINTECHCOM: Science, Technology and Communication Journal
Vol. 5, No. 1, October 2024, pp. 1-6, DOI: 10.59190/stc.v5i1.272

Plasma argon particle interactions in a non-equilibrium state through the Maxwell-Boltzmann kinetic equation

Azza Ronald[1], Saktioto[1,*], Kusherbayeva Maikul[2], Kushkimbayeva Bibara[2], Mohd Rendy Samudra[1], Yan Soerbakti[1], Dedi Irawan[3], Okfalisa[4]
[1]Department of Physics, Universitas Riau, Pekanbaru 28293, Indonesia
[2]Department of Physics and Informatics, M. Kh. Dulati Taraz State University, Taraz 12984, Kazakhstan
[3]Department of Physics Education, Universitas Riau, Pekanbaru 28293, Indonesia
[4]Department of Informatic Engineering, UIN Sultan Syarif Kasim, Pekanbaru 28293, Indonesia

ABSTRACT

Non-thermal Argon plasmas serve multiple functions, particularly in healthcare and industrial applications. Numerous particles of the same species exhibit varying velocities, referred to as a 'population'. The distribution function is a standard method for characterizing a population. The speed and energy distribution functions in the Maxwell-Boltzmann equation are simulated utilizing MATLAB. The density of each species was numerically calculated using the Runge-Kutta method. This research reviews various Argon species, including Ar*, Ar^+, Ar(1s5), Ar(1s4), Ar(1s3), Ar(1s2), Ar, and electrons. The parameters utilized include a pressure of 10 mTorr, an Argon temperature about 400 K, and an electron temperature about 30,000 K. The maximum velocity probability density value is observed in the Ar^+ species at 6.18 x 10^7 $(m/s)^{-1}$, while the minimum value is found in electrons at 1.93 $(m/s)^{-1}$. The maximum energy probability density value is observed in the Ar^+ species at 2.13 x 10^{29} $(Joule)^{-1}$, while the minimum value is found in the Ar(1s3) species at 1.40 x 10^{25} $(Joule)^{-1}$. The time evolution of the distribution function, independent of the coordinates *r*, is associated with *v*, at t = 10^{-8} s. The velocity distribution function is significantly affected by the density value, while the distribution function is contingent upon the velocity.

ARTICLE INFO

Article history:

Received Sep 29, 2024
Revised Oct 7, 2024
Accepted Oct 15, 2024

Keywords:

Argon
Density
Distribution
Non-Thermal
Plasma

This is an open access article under the CC BY license.

* **Corresponding Author**
E-mail address: saktioto@lecturer.unri.ac.id

1. INTRODUCTION

Plasma is utilized in the textile sector, lighting, electronics, and various other applications [1-2]. Research in the health sector indicates that non-thermal plasma can inactivate airborne viruses and generate sterile air. Industrial plasma technology employs a non-thermal plasma process that operates by transmitting electrical energy between two electrodes at pressures ranging from 10 to 1000 Pascals (Pa), far lower than the atmospheric pressure of 101325 Pa. This plasma, referred to as low-pressure plasma, is essential for fundamental research in the advancement of plasma technology [3-5]. Non-thermal plasma is a highly advanced technology now. This occurs because non-thermal plasma employs the principle of reactive gas, which can alter the surface qualities of materials or products without affecting their original bulk characteristics.

Plasma is a gas that is either partially or fully ionized, with its kinetic and potential energy influenced by the plasma's density, temperature, and pressure. Plasma exists in several forms in nature and can be categorized by temperature into thermal plasma and non-thermal plasma. Non-thermal plasma is a low-pressure plasma characterized by elevated electron temperatures and reduced temperatures of heavier particles (ions and neutral atoms) [6,7]. The temperature disparity between electrons and heavier particles is significant. In non-thermal plasma, the electron temperature can

attain 10,000-100,000 K (1-10eV), yet the gas temperature may approximate room temperature due to little collisions between electrons and particles. Non-thermal plasmas exhibit a low energy density [8-10].

Argon plasma is utilized for diverse applications, particularly in the healthcare and industrial domains. Argon was selected in the healthcare sector due to its biological inertness, low breakdown voltage, and cost-effectiveness [11,12]. In the industrial sector, Argon plasma was selected for its prevalent usage in cleaning, attributed to its widespread availability, capacity to inhibit oxidation, and cost-effectiveness [13,14].

In plasma, electrons exhibit a Maxwell distribution with varying kinetic energies compared to heavy particles, leading to the terms electron temperature (Te) for electrons and heavy particle temperature (Tg) for heavy particles. Plasma typically contains numerous particles of the same species exhibiting varying velocities, commonly referred to as a 'population' [15]. A prevalent method to characterize a population is by its distribution function f(x,v,t). The Maxwell-Boltzmann distribution is intricately connected to particle dynamics in gaseous or plasma states, governed by temperature and particle movement due to prevailing forces [16-18].

The Maxwell-Boltzmann Equation is employed to analyze particles in Argon plasma, facilitating the determination of the distribution of plasma particles, encompassing particle velocity distribution, particle energy distribution, and the temporal evolution of the distribution function. The density values for each species were calculated numerically with the Runge-Kutta method and can be computationally implemented using MATLAB software. The Runge-Kutta method yields solutions to differential equations with significantly reduced truncation error escalation.

Theoretical Review

Plasma comprises neutral or charged particles that generate an electromagnetic field, affecting the interactions among particles within the plasma system [19]. Plasma possesses distinct features in comparison to other states of matter. Plasma is deemed macroscopically neutral when it is unaffected by external influences, indicating that the plasma is in a state of equilibrium. A sufficiently substantial volume of plasma encompasses several particles, yielding minimal values for density and temperature. Measuring the electric field within the plasma yields a value of zero.

If macroscopic neutrality is not achieved, the potential energy contributed to the resultant Coulomb force will be significantly more than the kinetic energy of heat particles [20-21]. Secondly, the plasma temperature is directly proportional to the average kinetic energy of the particles [22]. The energy of an individual particle in kinetic or thermodynamic equilibrium arises from a Maxwell-Boltzmann distribution. Low-pressure plasmas utilized for glow discharge in the industrial sector frequently employ a non-Maxwellian electron energy distribution function. The average energy is quantified in Joules per particle; in gases that do not adhere to a Maxwellian distribution, it is equivalent to a Maxwellian distribution augmented by the effective kinetic temperature. The overall density of each particle species is only a function of time, independent of position [23], as seen in Equation (1)

$$n_\alpha = n_\alpha(t) \quad (1)$$

In the zero-dimensional framework, the continuity equation for the species reduces to the ordinary differential equation shown in Equation (2).

$$\frac{\partial n_\alpha}{\partial_t} = s_\alpha \quad (2)$$

Equation (2) appears straightforward; however, it is important to note that the source term s_α is dependent on temperature and the total density of other particle species. The source term for an α particle species is the aggregate of contributions from all reactions involving the species. The contribution $s_{\alpha r}$ indicates the number of particles of a species produced or consumed in reaction *r* per unit time [24].

Argon Plasma Characteristics and Interactions

Argon is a chemical element represented by the symbol Ar. An octet (eight electrons) signifies that the s and p subshells are fully occupied. Argon's complete outer electron shell renders it stable and highly resistant to bonding with other elements. The first ionization energy of Argon is 1520.6 kJ/mol.

Argon plasma comprise electrons, ions, and neutral atoms and can be generated through the ionization of gaseous particles [25]. Ionization is the process of extracting electrons from an atom or molecule, disrupting its bonds. The energy necessary to extract one or more electrons from their orbits in an atom or molecule is termed ionization energy (Ei). Recombination is the converse of ionization; during recombination, one or more electrons re-associate with atoms or molecules that are deficient in electrons (ions). Upon the capture of the electron by the ion, the atom or molecule will revert to a neutral state. In plasma, ionization and recombination occur rapidly and concurrently. The kinetic theory of gas posits that gas consists of a multitude of minute particles that exhibit random and perpetual motion. The universal ideal gas Equation is expressed as follows [9].

$$p = nk_BT \qquad (3)$$

The plasma state modifies the ideal gas laws. Global thermodynamic functions must be considered for each particle type. Reactive collisions alter the quantity of n particles. Equation (3) can be modified as given by

$$p = nk_BT - \frac{k_BT}{24\pi\lambda_D^3} \qquad (4)$$

Equation (4) indicates that the pressure of an ideal gas alters during its transition to plasma. The pressure of plasma can be consistently lower than that of an ideal gas [16].

Plasma exists in several forms in nature and can be categorized by temperature into thermal plasma and non-thermal plasma. Figure 1 illustrates the transition between thermal and non-thermal plasma.

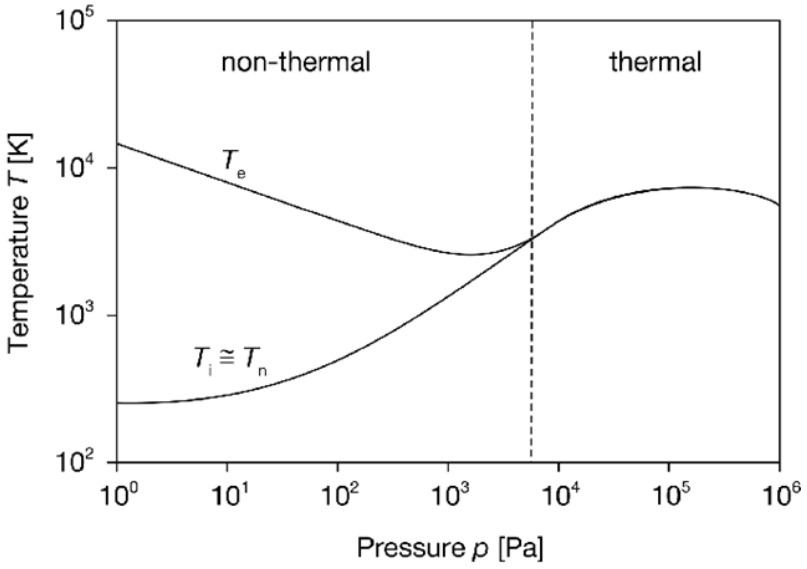

Figure 1. Transition between thermal and non-thermal plasma as a function of pressure [20].

Under cold plasma or non-thermal plasma circumstances, a non-Maxwellian distribution is applicable. Non-thermal plasma, or cold plasma, is a state of plasma characterized by a non-thermal equilibrium between the temperatures of the electrons and the gas. Figure 1 illustrates that the electron temperature is elevated, although the gas particle temperature remains comparatively low due to little collisions between electrons and gas particles.

Velocity distribution function

When particles let to interact and reach equilibrium, their velocities, and energy are dispersed throughout a spectrum of values characterized by the Maxwell-Boltzmann distribution function. In Cartesian coordinates (x, y, z), the quantity of particles dn_x within the velocity range from v_x to v_x+dv_x, where *n* denotes the particle density, is described by the one-dimensional Maxwell-Boltzmann distribution function [19].

$$f(v_x) = \frac{dn_x}{dv_x} = \frac{n}{\pi^{\frac{1}{2}}}\left(\frac{m}{2kT}\right)^{\frac{1}{2}} exp\left[-\frac{mv_x^2}{2kT}\right] \quad (5)$$

where *v* represents the radius vector within the velocity space of the spherical coordinate system. The velocity distribution dn_v between *v* and *v+dv* is represented by the distribution function for velocity *v*, i.e.,

$$f(v) = \frac{dn_v}{dv} = \frac{4n}{\pi^{\frac{1}{2}}}\left(\frac{m}{2kT}\right)^{\frac{3}{2}} exp\left[-\frac{mv^2}{2kT}\right] \quad (6)$$

Given the symmetry f(v), we can integrate the solid angle to express the probability distribution of velocity as a function [19].

$$f(v) = \left(\frac{m}{2\pi kT}\right)^{\frac{3}{2}} 4\pi n v^2 e^{-\frac{mv^2}{2kT}} \quad (7)$$

Energy Distribution Function

The energy of individual particles in a gas in kinetic or thermodynamic equilibrium conforms to the Maxwell-Boltzmann distribution. Kinetic energy *E* can be defined with speed *v* as

$$E \equiv \frac{1}{2}mv^2 \quad (8)$$

then the energy distribution between *E* and *E* + *dE* is

$$f(E) = \frac{dn_E}{dE} = \frac{2n}{\pi^{\frac{1}{2}}}\frac{E^{\frac{1}{2}}}{(kT)^{\frac{3}{2}}} exp\left[-\frac{E}{kT}\right] \quad (9)$$

The energy distribution function of a particle is characterized by the Maxwell-Boltzmann distribution when the particle is in thermodynamic or kinetic equilibrium. Thermodynamic equilibrium is the most rigorous condition, indicating that all energy transfers within the gas are negligible, the mean free path of photons is considerably less than the gas dimensions, and the gas emits radiation akin to a black body. Thermodynamic equilibrium is both a required and sufficient condition for the effective application of traditional thermodynamic methods to gases. Kinetic equilibrium is a more stringent condition that permits energy to transfer inside the medium without necessitating that the medium emit radiation akin to a black body. Kinetic equilibrium necessitates sufficient particle interaction to attain a Maxwell-Boltzmann velocity distribution [19].

The solution of the Maxwell-Boltzmann Kinetic Equation uses the 4th Order Runge-Kutta method. This method provides solutions to differential Equations with much-reduced truncation error accumulation. The Runge-Kutta method is commonly employed to address numerical calculation issues [25]. The standard representation of the fourth-order Runge-Kutta technique is as follows:

$$y_{i+1} = y_i + h(a_1k_1 + a_2k_2 + a_3k_3 + a_4k_4) \quad (10)$$

where a_1, a_2, ..., an are constants, *h* represents the step size for each iteration, and *n* denotes the method order. In the context of the 4th order Runge-Kutta method, the values of k_1, k_2, k_3, and k_4 are: [10,25]

$$k_1 = f(t_i, y_i) \quad (11)$$

$$k_2 = f(t_i + p_1 h\,, y_i + q_{11} k_1 h) \quad (12)$$

$$k_3 = f(t_i + p_2 h\,, y_i + q_{21} k_1 h + q_{22} k_2 h) \quad (13)$$

$$k_4 = f(t_i + p_3 h\,, y_i + q_{31} k_1 h + q_{32} k_2 h + q_{33} k_3 h) \quad (14)$$

1. Research Methods

The features of Argon plasma were modeled computationally using MATLAB software. The process has three phases. The initial phase commences with a review encompassing plasma properties, features of Argon gas, and a compilation of Argon plasma response data. The subsequent phase involves constructing a model based on the employed mathematical formulae. The subsequent phase involves developing a simulation utilizing Matrix Laboratory. The arrangement of plasma particle interactions is determined by the Maxwell-Boltzmann distribution Equation. The Runge-Kutta method will be employed for density calculations of each species. The mathematical Equation model will be input into the MATLAB programming environment. Table 1 presents a compilation of Argon plasma reaction data.

Tabel 1. Rection for Argon plasma

Reaksi	Cross Section (m^2)	ΔE (eV)	
e + Ar → e + Ar*	5,43 x10^{-23}	11,55	[7]
e + Ar → 2e + Ar^+	2,02 x10^{-22}	15,76	[7]
e + Ar → e + Ar(1s5)	5,916 x10^{-23}	11,54	[14]
e + Ar → e + Ar(1s4)	4,648 x10^{-23}	11,62	[14]
e + Ar → e + Ar(1s3)	8,45 x10^{-24}	11,78	[14]
e + Ar → e + Ar(1s2)	4,225 x10^{-23}	11,87	[14]
e + Ar → e + Ar	7,5 x10^{-20}	13,6 x10^{-6}	[7]

The simulation program script comprises *kreaksi.m*, *ndensitas.m*, *odefun.m*, *xkecepatan.m*, *xenergi.m*, and *xtimeev.m*. *Kreaksi.m* calculates coefficients for each reaction, *ndensitas.m* and *odefun.m* compute density for each species based on the derived coefficients, *xkecepatan.m* and *xenergi.m* analyze speed and energy distributions according to Maxwell-Boltzmann Equations, and *xtimeev.m* facilitates the time evolution of the distribution function.

The reaction data program comprises a compilation of cross-section and energy values for each reaction, which will be automatically accessed by Matlab using the 'Import Data' function. The data will be analyzed to ascertain the reaction coefficient, subsequently yielding the density value for each species. The distribution function software comprises two components: *xkecepatan.m* and *xenergi.m.* Both distribution function algorithms commence with the input of the physical constant values, specifically the particle mass, Boltzmann constant, Argon temperature, electron temperature,

and pressure. The initial input data comprises boundary conditions represented by speed or energy values and density input values for each species. The time evolution program commences with the input of physical constants, specifically the particle mass, Boltzmann constant, and collision frequency. The first input data comprises boundary conditions represented by time interval and speed interval values.

2. Results And Discussion

Non-Termal Argon Species

The coefficient values for each reaction based on cross-section and energy data can be seen in Table 2.

Tabel 2. Coefficient values for each reaction

Reaction	Reaction Coefficient (m^3/s)
$e + Ar \rightarrow e + Ar^*$	$3{,}68 \times 10^{-17}$
$e + Ar \rightarrow 2e + Ar^+$	$1{,}17 \times 10^{-04}$
$e + Ar \rightarrow e + Ar(1s5)$	$1{,}29 \times 10^{-16}$
$e + Ar \rightarrow e + Ar(1s4)$	$2{,}72 \times 10^{-09}$
$e + Ar \rightarrow e + Ar(1s3)$	$6{,}20 \times 10^{-14}$
$e + Ar \rightarrow e + Ar(1s2)$	$1{,}11 \times 10^{-08}$
$e + Ar \rightarrow e + Ar$	$4{,}41 \times 10^{-08}$

The density value for each species is calculated based on the reaction coefficient value of each reaction. The values of parameters used in this modeling are presented in Table 3.

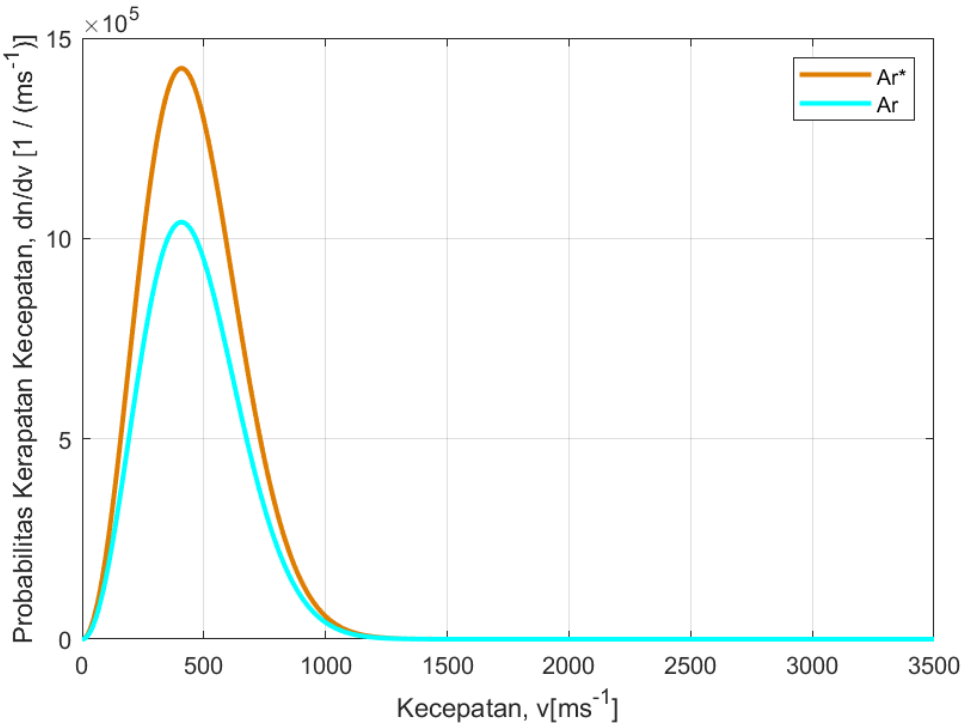

Figure 2. Particle speed distribution Ar^*dan Ar.

Tabel 3. Density and mass values of each species.

	Spesies							
	Ar^*	Ar^+	Ar $1s5$	Ar $1s4$	Ar $1s3$	Ar $1s2$	Ar	e
n_0 (m^{-3})	7x 10^8	10^5	10^7	9,0x10^6	2x 10^6	4,00 x10^6	5x 10^8	5 x10^5
n (m^{-3})	7x 10^8	3,04x 10^{10}	10^7	9,7x10^6	2x 10^6	6,88 x10^6	5,11x10^8	6,07x 10^{10}
m (kg)	6,63 x 10^{-26}							9,1 x 10^{-31}

Velocity distribution of Argon particles from the Maxwell-Boltzmann kinetic Equation

The constituent particles of standard plasma do not exhibit uniform velocities. When particles are let to interact and equilibrate, their velocities are dispersed across a spectrum of values characterized by the Maxwell-Boltzmann distribution function. The area beneath each velocity distribution curve corresponds to the particle density. The velocity distribution is contingent upon the gas temperature and the response coefficient. Figure 2 illustrates the velocity distribution for Ar* and Ar.

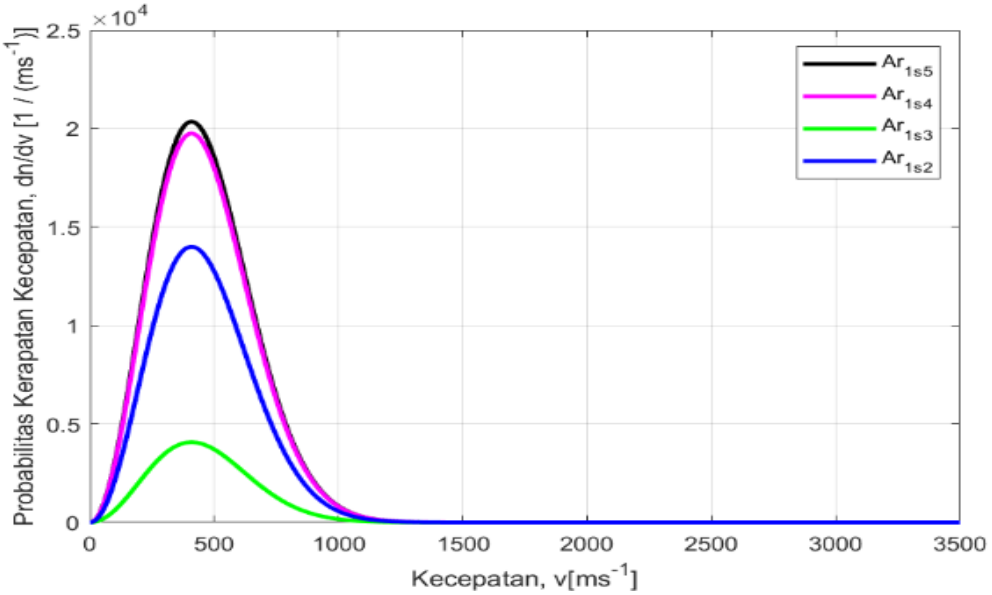

Figure 3. Velocity distribution of particle $Ar(1s5)$, $Ar(1s4)$, $Ar(1s3)$, dan $Ar(1s2)$.

Figure 2 indicates that the probability value of the speed density for the species Ar* is 1.42 x 10^6 $(m/s)^{-1}$, whereas the probability value for the species Ar is 1.04 x 10^6 $(m/s)^{-1}$. The disparity in value among species is 3.84 x 10^5 $(m/s)^{-1}$. The elevated maximum value of the probability density speed of the Ar* species results from these particles transitioning to a higher shell and absorbing kinetic energy due to temperature, resulting in a significantly high speed of the Ar* particles. The excited state will revert to its original state by emitting photons, resulting in a decline of the curve. Concurrently, Ar

particles possess a lower density than Ar*, which corroborates the assertion that the area beneath each velocity distribution curve is equivalent to the particle density.

The effective lifetime of Argon atoms in metastable states, 1s5 and 1s3 (in Paschen notation), in non-thermal plasmas is significantly influenced by their collisional transfer to resonant states (1s2 and 1s4) [4,8]. Figure 3 illustrates the velocity patterns of Ar(1s5), Ar(1s4), Ar(1s3), and Ar(1s2).

Figure 3 presents the probability values of the velocity density for the species Ar(1s5) at 2.03 x 10^4(m/s)$^{-1}$, Ar(1s4) at 1.97 x 10^4(m/s)$^{-1}$, Ar(1s3) at 4.07 x 10^3(m/s)$^{-1}$, and Ar(1s2) at 1.4 x 10^4(m/s)$^{-1}$. The peak values of the probability density of speed differ as follows: 6.00 x 10^2(m/s)$^{-1}$, 5.75 x 10^3(m/s)$^{-1}$, and 9.93 x10^3(m/s)$^{-1}$. The graph illustrates the correlation between speed density probability and the density of individual particles. The species Ar(1s3) is obtained from the density of states Ar(1s5), and the species Ar(1s2) is derived from Ar(1s4) according to the ratios of nAr(1s3) = nAr(1s5)/10 and nAr(1s2) = nAr(1s4)/4.

Low-pressure plasma, density is low, resulting in infrequent heavy particle collisions, while electron collisions are significant [4]. Figure 4 illustrates the velocity distribution of Ar^+ ions and electrons.

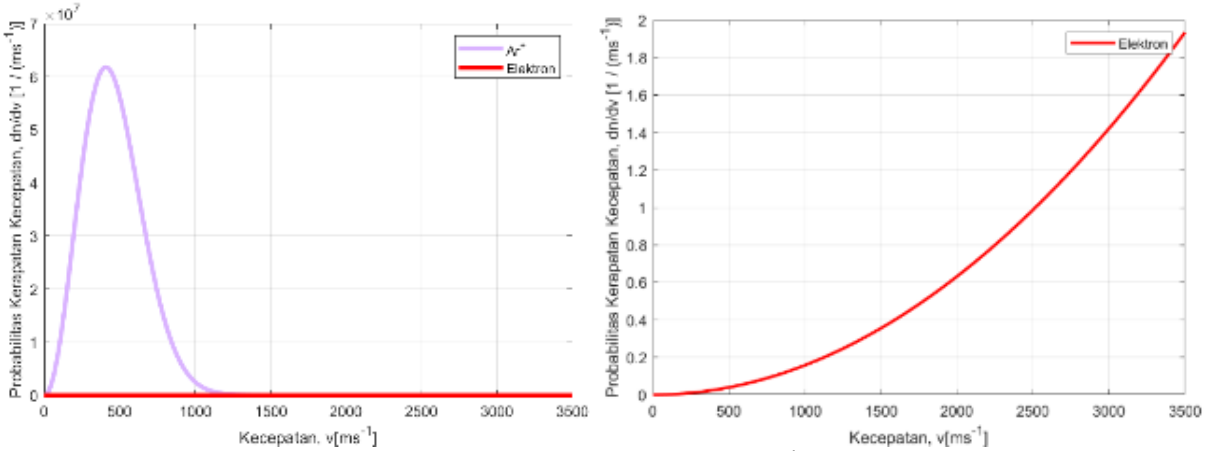

Figure 4. Velocity distribution of particle (a) Ar^+ and (b) electron

Figure 4 indicates that the probability value of the speed density for Ar^+ species is 6.18 x10^7(m/s)$^{-1}$, whereas the probability value for the speed density of electrons is 1.93 (m/s)$^{-1}$. The electron speed distribution graph exhibits an exponential form, indicating that an increase in speed results in minimal changes to the probability density, primarily due to the influence of other significant factors. The value of significant disparity results in the probability of the electron velocity density approaching a constant state. Compared to Ar and Ar*, the species Ar^+ exhibits a relatively high probability. The recombination process occurs during collisions, enabling Ar^+ to merge with other particles, which leads to a reduction in the curve.

Argon plasma energy distribution from the Maxwell-Boltzmann Equation

The energy distribution of individual particles in a gas adheres to the Maxwell-Boltzmann distribution. The energy density probability is affected by the particle's density, velocity, and mass. Figure 5 illustrates the energy distribution function for Ar* and Ar.

Figure 5 indicates that the probability value of the energy density for the species Ar* is 4.91 x 10^{27} (Joule)$^{-1}$, whereas the probability value for the species Ar is 3.59 x 10^{27} (Joule)$^{-1}$. The value difference between species is 1.32 x 10^{27} Joule^{-1}. The elevated maximum value of the probability energy density of Ar* is attributed to the energy of these particles to their velocity. The excited state will revert to its ground state through the emission of photons, resulting in a decline of the curve. In contrast, Ar particles exhibit a lower velocity compared to Ar*. Excitation refers to the process in which electrons transition from a lower energy level to a higher energy level resulting in energy absorption during a collision with another electron. The event opposite to excitation is termed relaxation or deexcitation, which is associated with the emission of photons. Ionized gas does not necessarily qualify as plasma. Figure 6 illustrates the energy distribution graph for Ar(1s5), Ar(1s4), Ar(1s3), and Ar(1s2).

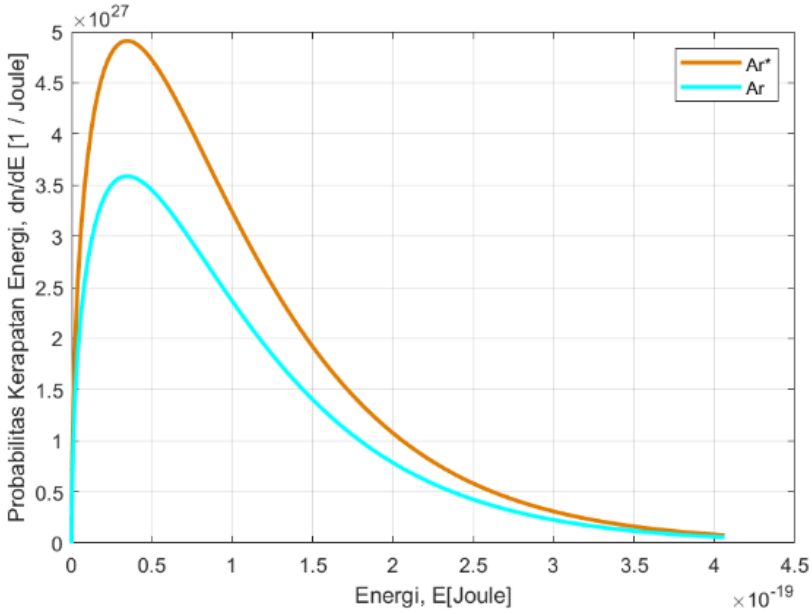

Figure 5. Energy distribution of species Ar^* and Ar.

Figure 6 presents the probability values of the energy density for the species Ar(1s5) at 7.01×10^{25} (Joule)$^{-1}$, Ar(1s4) at 6.81×10^{25} (Joule)$^{-1}$, Ar(1s3) at 1.40×10^{25} (Joule)$^{-1}$, and Ar(1s2) at 4.82×10^{25} (Joule)$^{-1}$. The variation in the peak value of the energy density probability from the highest value is 2.07×10^{24} (Joule)$^{-1}$, 1.98×10^{25} (Joule)$^{-1}$, and 3.42×10^{25} (Joule)$^{-1}$. Argon absorbs energy until it reaches a specific threshold. Upon reaching this maximum, it can no longer absorb external energy and begins to emit photons, resulting in a decline in the energy function.

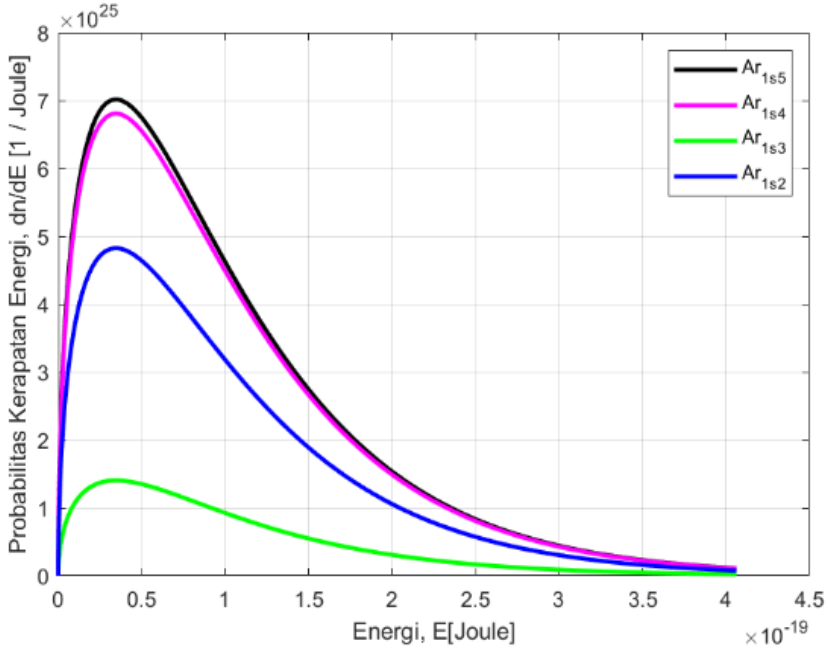

Figure 6. Energy distribution of spesies $Ar(1s5)$, $Ar(1s4)$, $Ar(1s3)$, dan $Ar(1s2)$.

In low-pressure plasma, the density is low, resulting in infrequent heavy particle collisions, while electron collisions are significant [4]. Figure 7 illustrates the energy distribution graph for Ar^+ ions and electrons.

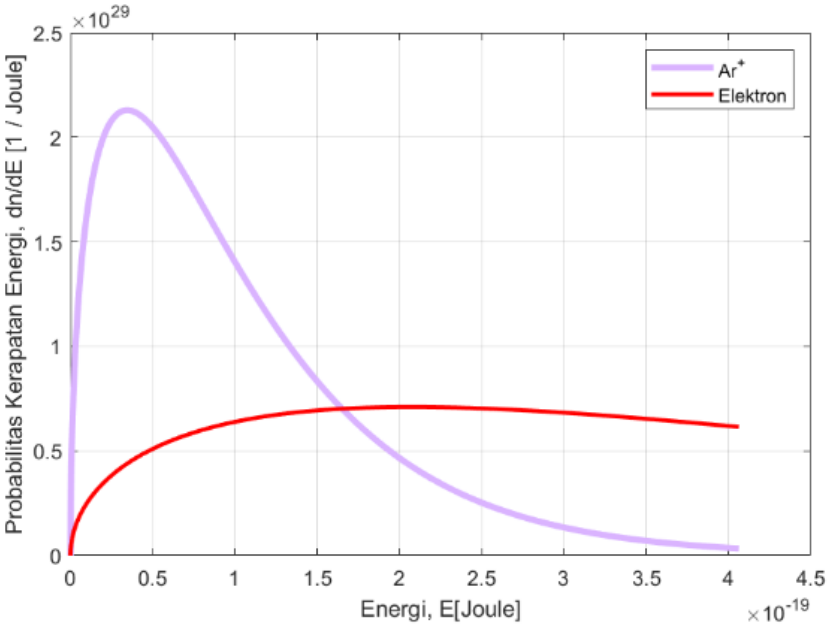

Figure 7. Energy distribution of spesies Ar^+ and electron.

Figure 7 indicates that the probability value of the energy density for the species Ar^+ is 2.13 x 10^{29} $(Joule)^{-1}$, whereas the probability value for the energy density of electrons is 7.10 x $10^{29}(Joule)^{-1}$. The electron energy distribution function remains relatively constant, as the electrons are external to the Argon group and can be classified as free electrons. When the energy of the electrons is maximized, external energy will seek to stabilize the heavier particles, specifically Argon, resulting in energy absorption by these particles.

Time evolution over the velocity distribution function

In the time evolution program of the distribution function, it is assumed that space is homogeneous, meaning the distribution function is independent of the coordinate *r*. However, the distribution function may also exhibit anisotropy, indicating that it can depend on the velocity vector *v*, rather than solely on its magnitude. The program utilizes the fundamental non-equilibrium formulation of the kinetic Boltzmann equation. Figure 8 illustrates the time evolution of the speed distribution function.

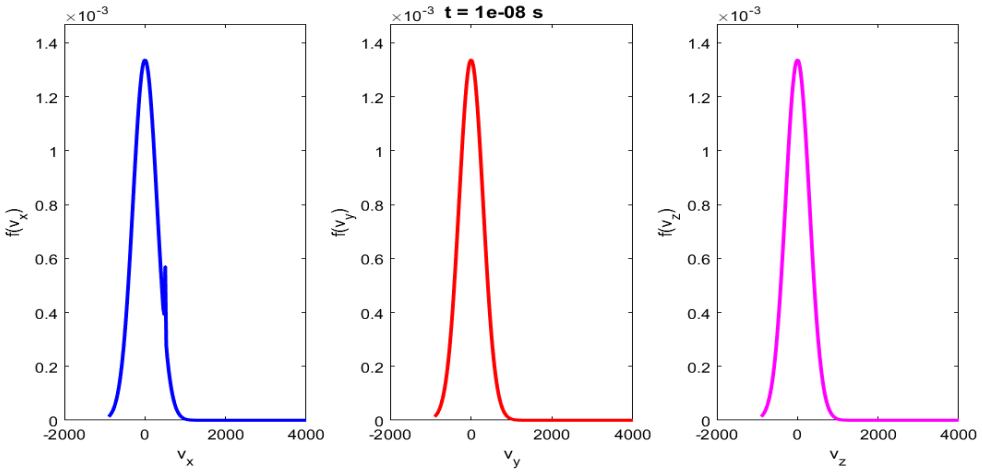

Figure 8. Time evolution over velocity distribution function

Figure 8 indicates that this approach presumes the external force acting on the particle is null. The program does not solve the differential Equation; it merely provides a visual representation of the

solution [17]. At 10^{-8} seconds, the Argon plasma is in a state of nonequilibrium and is approaching its equilibrium condition.

3. Conclusion

The research and analysis derived from simulations of particle velocity and energy distribution in non-thermal plasma indicate a strong correlation between particle velocity density and the density, mass, and temperature of each species. The species Ar* and Ar exhibited peak values of $1.42x10^{6}(m/s)^{-1}$ and $1.04x10^{6}(m/s)^{-1}$, respectively. The elevated value for both species can be attributed to their density. The peak values for the species Ar(1s5), Ar(1s4), Ar(1s3), and Ar(1s2) are 2.03×10^{4} $(m/s)^{-1}$, 1.97×10^{4} $(m/s)^{-1}$, $4.07 \times 10^{3}(m/s)^{-1}$, and $1.4 \times 10^{4}(m/s)^{-1}$, respectively. This phenomenon is attributed to the density relationship Ar(1s5) > Ar(1s4), with n Ar(1s3) equating to n Ar(1s5)/10, and n Ar(1s2) corresponding to n Ar(1s4)/4. In the species Ar^ and electrons, the respective velocities are 6.18×10^{7} m/s and 1.93 m/s. The probability of particle energy density is intricately linked to the velocity and density of each species. The species Ar* and Ar exhibited peak values of $4.91x10^{27}(Joule)^{-1}$ and $3.59x10^{27}$ $(Joule)^{-1}$, respectively. The peak values for the species Ar(1s5), Ar(1s4), Ar(1s3), and Ar(1s2 are 7.01×10^{25} $Joule^{-1}$, 6.81×10^{25} $Joule^{-1}$, 1.40×10^{25} $Joule^{-1}$, and 4.82×10^{25} $Joule^{-1}$, respectively. For the species Ar^{+} and electrons, the respective values are 2.13×10^{29} $(Joule)^{-1}$ and $7.10 \times 10^{28}(Joule)^{-1}$. The time evolution of the distribution function in non-thermal Argon plasma is independent of the coordinate *r* and is associated with *v*, with a value of $t = 10^{-8}$ s.

Acknowledgment

The author acknowledges DRTPM for its financial support of this research in 2024. Appreciation is expressed to LPPM Riau University and the Plasma and Computational Physics Laboratory for their support and provision of laboratory facilities used in this research, as well as to M.H. Dulati from Taraz University, Kazakhstan, for collaborative discussions regarding the results.

References

1. Alves, L. L., Bogaerts, A., Guerra, V., & Turner, M. M. (2018). Foundations of modelling of nonequilibrium low-temperature plasmas. *Plasma Sources Science and Technology*, *27*(2). https://doi.org/10.1088/1361-6595/aaa86d
2. Baeva, M., Bösel, A., Ehlbeck, J., & Loffhagen, D. (2012). Modeling of microwave-induced plasma in argon at atmospheric pressure. *Physical Review E - Statistical, Nonlinear, and Soft Matter Physics*, *85*(5), 1–9. https://doi.org/10.1103/PhysRevE.85.056404
3. Bárdos, L., & Baránková, H. (2010). Cold atmospheric plasma: Sources, processes, and applications. *Thin Solid Films*, *518*(23), 6705–6713. https://doi.org/10.1016/j.tsf.2010.07.044
4. Carbone, E., Van Veldhuizen, E., Kroesen, G., & Sadeghi, N. (2015). Electron impact transfer rates between metastable and resonant states of argon investigated by laser pump-probe technique. *Journal of Physics D: Applied Physics*, *48*(42). https://doi.org/10.1088/0022-3727/48/42/425201
5. D'Ammando, G., Colonna, G., Pietanza, L. D., & Capitelli, M. (2010). Computation of thermodynamic plasma properties: A simplified approach. *Spectrochimica Acta - Part B Atomic Spectroscopy*, *65*(8), 603–615. https://doi.org/10.1016/j.sab.2010.05.002
6. Fridman, G., Fridman, A., Gutsol, A., Vasilets, V., & Friedman, G. (2007). *Comparison of Direct and Indirect Effects of Non-Thermal Atmospheric Pressure Plasma on Bacteria and Mechanisms of Such Interaction*. *November 2014*, 322–322. https://doi.org/10.1109/ppps.2007.434562
7. Hayashi, M. (2003). *NIFS-DATA Series*.
8. Karnopp, J., Magaldi, B., Sagás, J., & Pessoa, R. (2022). The Effect of Excited Species on the Collisional Energy of Argon Inductively Coupled Plasmas: A Global Model Study. *Plasma*, *5*(1), 30–43. https://doi.org/10.3390/plasma5010003
9. Krall, N. A., Trivelpiece, A. W., & Gross, R. A. (1973). Principles of Plasma Physics. *American Journal of Physics*, *41*(12), 1380–1381. https://doi.org/10.1119/1.1987587
10. Lestari, R. N. (2019). *Metode Runge Kutta Orde 4 pada Model Penyebaran Influenza dengan Populasi SIRC*. 55.

11. Matthias, Z. (2008). Argon plasma coagulation therapy. *GMS Krankenhaushyg Interdiszip*, *3(1)*(5), 612–616. https://doi.org/10.1097/MOG.0b013e32830bf825
12. Melero, C., Rincón, R., Muñoz, J., Zhang, G., Sun, S., Perez, A., Royuela, O., González-Gago, C., & Calzada, M. D. (2018). Scalable graphene production from ethanol decomposition by microwave argon plasma torch. *Plasma Physics and Controlled Fusion*, *60*(1). https://doi.org/10.1088/1361-6587/aa8480
13. Mishra, R., & Trivedi, H. (2016). *Cold Plasma : Emerging As the New Standard in Food Safety Cold Plasma : Emerging As the New Standard in Food Safety Ritesh Mishra *, Sunny Bhatia , Ramesh Pal , Amit Visen and Himanshu Trivedi*. *6*(2). https://www.researchgate.net/publication/343532073%0ACold
14. Napartovich, A., Dyatko, N., Kochetov, I., & Sukharev, A. (2017). Electron Energy Distribution Function. *The State Science Center Troitsk Institute for Innovation and Fusion Reseacrh*.
15. Norman, G. E., & Timofeev, A. V. (2011). Kinetic temperature of dust particle motion in gas-discharge plasma. *Physical Review E - Statistical, Nonlinear, and Soft Matter Physics*, *84*(5), 1–13. https://doi.org/10.1103/PhysRevE.84.056401
16. Nur, M. (2011). *Fisika Plasma dan Aplikasinya*. Universitas Diponegoro.
17. Panesi, M. (2009). Physical models for nonequilibrium plasma flow simulations at high speed re-entry conditions. *October*.
18. Pastor-Pérez, L., Belda-Alcázar, V., Marini, C., Pastor-Blas, M. M., Sepúlveda-Escribano, A., & Ramos-Fernandez, E. V. (2018). Effect of cold Ar plasma treatment on the catalytic performance of Pt/CeO2 in water-gas shift reaction (WGS). *Applied Catalysis B: Environmental*, *225*, 121–127. https://doi.org/10.1016/j.apcatb.2017.11.065
19. Reece, J. (1995). *Industrial Plasma Engineering* (Vol. 1). http://cds.cern.ch/record/1139914/files/9780471720010_TOC.pdf%0Ahttp://files/261/253714985_Principles_of_Plasma_Discharges_and_Materials_Processing_2nd_Edition.html
20. Roth, C., Sonnenfeld, A., & Rudolf Von Rohr, P. (2011). Nanoscale plasma surface modification of powders. *Technical Proceedings of the 2011 NSTI Nanotechnology Conference and Expo, NSTI-Nanotech 2011*, *1*(20812), 225–228.
21. Saktioto, T., Nawi, N. D., Ismail, F. D., & Farma, R. (2017). Performance of pinching radius effects to current densities of NX2 plasma focus. *Advanced Studies in Theoretical Physics*, *11*(12), 551–559. https://doi.org/10.12988/astp.2017.689
22. Tendero, C., Tixier, C., Tristant, P., Desmaison, J., & Leprince, P. (2006). Atmospheric pressure plasmas: A review. *Spectrochimica Acta - Part B Atomic Spectroscopy*, *61*(1), 2–30. https://doi.org/10.1016/j.sab.2005.10.003
23. Tota Pirdo Kasih, & Nasution, J. (2014). Pengembangan Teknologi Plasma Dingin Untuk Modifikasi Karakteristik Permukaan Material Tanpa Mengubah Sifat Dasar Material. *Jurnal PASTI*, *X*(3), 373–379.
24. Yiğit, E. (2018). *Erratum to: Atmospheric and Space Sciences: Ionospheres and Plasma Environments*. E1–E1. https://doi.org/10.1007/978-3-319-62006-0_6
25. Zealand, N. (1996). *history of Runge-Kutta methods*. *20*, 247–260.